A Novel Electromagnetic Active Contact Flange Design for Robotic Polishing

H. I. Lin, *Member, RST* and Y. H. Chen, *Member, RST*

***Abstract*—This study proposes a new electromagnetically driven active contact flange design in which a magnetic field is used as the source of the contact force and the characteristics of the mechanical structure are leveraged to overcome the problem of insufficient rotating motor flexibility. The proposed flange was verified experimentally, and the results revealed that it exhibited a faster transient response time, more stable contact force control, and less noise disturbance when compared with the conventional design. Furthermore, an optimization method was developed to compensate for the nonlinearity of the magnetic field under varying flange positions. The proposed active contact flange is suitable for delicate polishing tasks.**

***Index Terms*—Active contact flange; magnetic field; polishing.**

I. Introduction

In many industrial applications, surface polishing processes such as grinding, sanding, and polishing are used in the finishing stage to reduce surface roughness [1]. Currently, industrial robots are used to perform the polishing process to reduce the cost of labor and to improve efficiency and quality [2]. The quality of polishing is based on the control of the contact force, and contact flanges can effectively control the contact force; thus, contact flanges have been commonly used in polishing processes. Contact flanges can be divided into two types according to whether the flange is controlled: active contact flanges (ACFs) and passive contact flanges [3]. Passive contact flanges commonly involve spring mechanisms, but the spring oscillation engenders challenges in maintaining a stable contact force [4] [5]. ACFs were developed to overcome this problem, including the FerRobotics ACF Kit, ATI PCFC, and PushCorp AFD; moreover, ACFs use pneumatic pressure as a power source [6]. The use of a pneumatic power source enables the contact force to be adjusted through air pressure measurement [7]. However, ACFs have several disadvantages; for example, ACFs are expensive to maintain and are noisy, and the compressibility of the air results in a relatively long transient response time of the force control system [8].

Computer numerical control machining has the advantages of rigidity and precision. These properties are crucial for automatic polishing, which requires precise and rapid force control [9]. The quality of polishing is affected by multiple factors, such as the grinding particle size, tool path, contact force, tool wear, feed rate, and rotational speed [10]. Several studies have shown that contact force is a key factor affecting the roughness of a polished surface [11] [10] [6].

Usually, force control methods in robotic polishing uses multiple joint motors of a robot to regulate the force [12]. Nevertheless, systems with multiple motors respond more slowly than do those with a single motor due to the high inertia, which causes severe vibrations, consequently leading to more energy consumption. To avoid surface damage caused by excessive polishing, industrial robotic polishing systems require variable and responsive contact flanges [11]. Whitney [3] proposed two main approaches for contact force control: passive compliance control and active compliance control. Because passive compliance control methods are not suitable for high-precision polishing operations, active compliance control methods are used [13]. Accordingly, this study proposes a new ACF design involving the use of a voice coil motor (Fig. 1).

The remainder of this paper is organized as follows. In Section II, the static performance of a pneumatic contact flange is explained and compared with our proposed electromagnetically driven ACF. In Section III, a contact force optimization method based on a force-constant model is proposed for obtaining stable contact quality rapidly in order to solve the problems of magnetic field attenuation and nonlinear force constants during voice coil motor movement. In Section IV, simulations and experiments are presented to validate the feasibility and effectiveness of the proposed ACF.

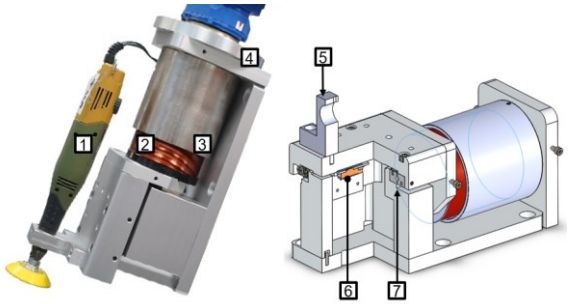

Fig. 1. Structure diagram of the proposed ACF (1)Polishing tool (2)Motor mover (3)Motor stator (4)Upper flange(5)Grinding holder (6)Grating scale and IMU sensor (7)Linear slide

II. Comparison Of Pneumatic And Magnetic Field Methods

A. Transient analysis of contact flanges

The time required to reach a stable contact state depends on the transient time of the contact force control method. In addition, rapid dynamic control is achieved with a high response speed. This study conducted an experiment to measure the transient state and performance of the contact flange. In the experiment, a force sensor and a contact flange were installed on a milling cutter seat and the platform of a milling machine, respectively. The thrust direction of the contact flange was calibrated to ensure that the contact force was perpendicular to

H. I. Lin, is a Professor with National Yang Ming Chiao Tung University, Hsinchu, TAIWAN 30010. (e-mail: sofin@nycu.edu.tw).

Y. H. Chen is a Research Assistant with National Yang Ming Chiao Tung University, Hsinchu, TAIWAN 30010. (e-mail: t109618005@ntut.org.tw).

the force sensor. A weight holder was installed on the moving end to simulate load changes with different tool installations. Fig. 2 illustrates the experimental setup.

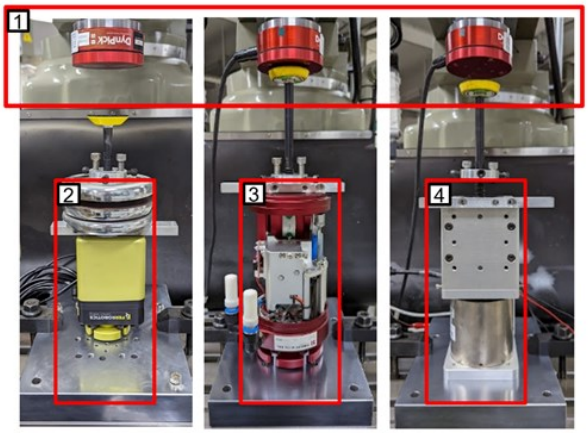

Fig. 2. Experimental setup for transient analysis (1)Force sensor (2)Pneumatically (3)Pneumatically (4)Magnetic

The total mass of the mover can be expressed as follows:

$$M_{tol} = M_B + M_T \tag{1}$$

Where M_B is the net weight of the mover and M_T is the tool payload. The mass of the mover changes as the load increases. Fig. 3 shows that the effect of gravity on the mass of the mover changes with the tilt angle (Fig. 3).

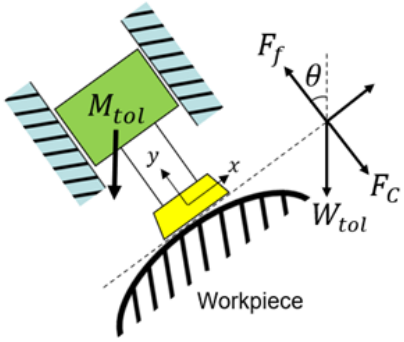

Fig. 3. Schematic of the analysis of the force of the compliant device

The static force can be expressed as follows:

$$\begin{aligned} F_{cont} &= M_{tol} g \cos\theta + F_C - F_f \\ &= W_{tol} \cos\theta + F_C - F_f \end{aligned} \tag{2}$$

where θ is the angle between the normal direction of the surface and the direction of gravity, F_C is the normal contact force of the workpiece, and F_f is friction between the mover and the stator.

B. *Transient analysis*

When the static resultant force Fcont is positive, the mover makes contact with the force sensor in the positive direction; however, if it is in the opposite direction from the workpiece, the mover does not make contact with the device. An increase in kinetic energy engenders an increase in the speed of the mover. The work and kinetic energy can be derived as follows:

$$W = F_C \cdot S \tag{3}$$

$$E_k = \frac{1}{2} M_{tol} v^2 \tag{4}$$

where v is the velocity of the y-axis, and S is the displacement of the y-axis.

When the static resultant force is positive, the mover eventually makes contact with the force sensor, at which point the force sensor records data regarding changes in the force, which can be used to observe the device's transient control characteristics. In addition, if the mass of the mover is increased through the addition of loads, the corresponding increase in the kinetic energy of the mover must be balanced out at the moment of contact, and this is directly reflected in the maximum capability of the force sensor (Fig. 4).

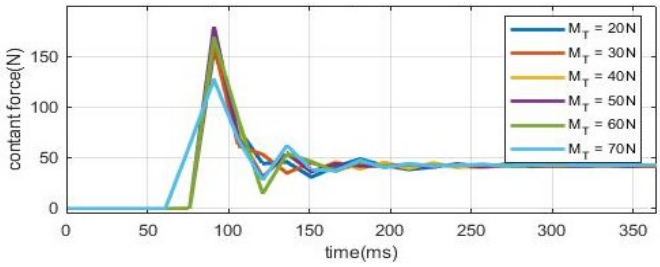

Fig. 4. Transient response

C. *Steady-state errors*

As illustrated in Fig. 4, the voice coil motor is always in contact with the sensor, and this can effectively reduce changes in the relative position between the polishing tool and the workpiece and reduce unnecessary work in the normal direction, which is useful for precision polishing. To evaluate the influence of kinetic energy on control performance, this study considered the mass of the mover as the experimental variable and considered the static resultant force and the y-axis displacement as the control variables.

Fig. 5 displays the original unfiltered sensor data. The voice coil motor maintained a fairly stable magnetic field after making contact with the force sensor. Under different loading conditions, the steady-state error was easily maintained within 0.5 N, which is closely related to the winding method of the coil and the stability advantage of the permanent magnetic field [7]. These findings indicate that the proposed electromagnetically driven contact device has a shorter transient response time, more stable contact force control, and better dynamic response performance. Nevertheless, it still has some obvious problems. The expected steady-state output slightly shifted under different loads (Fig. 5).

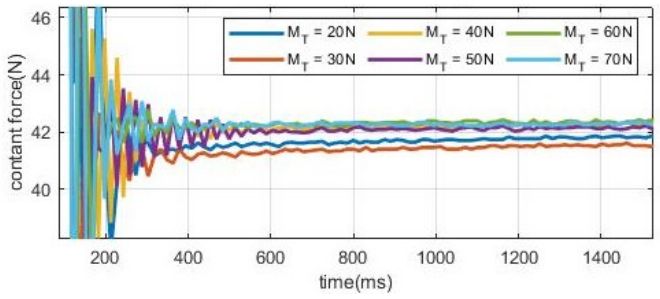

Fig. 5. Steady-state errors observed in the study

III. Design Of Electromagnetically Driven Contact Devices

A. *Control system*

The steady-state errors and transient problems described in the preceding section must be addressed before the pneumatic contact flange can be used for precise contact control. This section presents a discussion of the magnetic drive system and a verification of the advantages of the voice coil motor, such as its fast dynamic response speed and high control accuracy [14].

During the polishing process, the voice coil motor acts as the driving device to control the contact force by adjusting the current. Fig. 6 illustrates the system structure of the proposed ACF, indicating that the proposed ACF contains a voice coil motor, a grating scale, and a motor driver. The stator end of the voice coil motor is installed on the end of the industrial robot. The mover is connected to the polishing tool, and the stator and the mover move linearly along the linear slide rail.

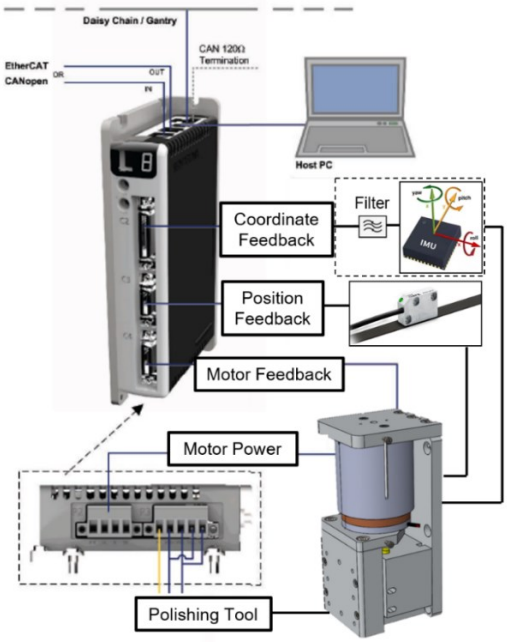

Fig. 6. Proposed system structure

B. *Magnetic field theory formulas*

When current flows through a metal wire, a magnetic field is generated around the wire. The generated magnetic field is proportional to the magnitude of the current. If the wire thickness is not considered, the strength of a magnetic field around a wire can be derived as follows:

$$B = \frac{\mu I}{2\pi r}, r \geq R \tag{5}$$

where μ is the constant $4\pi \cdot 10^{-7}\ \frac{T \cdot m}{A}$, I is the current, and r is the shortest distance to the wire.

When the wire is circular, the strength of the magnetic field at the centre of the wire can be derived as follows:

$$B = \frac{\mu I R^2}{2(R^2 + z^2)^{\frac{3}{2}}} \tag{6}$$

where R is the radius of the wire and z is the distance from the wire.

When multiple circular wires are combined into a solenoid, the strength of the magnetic field at the centre of the wire can be derived as follows:

$$B = \frac{\mu n I}{L}\left\{\frac{L + 2x}{2\lceil D^2 + (L + 2x)^2\rceil^{\frac{1}{2}}} + \frac{L - 2x}{2\lceil D^2 + (L - 2x)^2\rceil^{\frac{1}{2}}}\right\} \tag{7}$$

where L is the length of the solenoid, D is the diameter of the solenoid, and x is the distance from point P on the central line of the solenoid to the central point of the central line.

Numerous types of voice coil motors are available. Under normal conditions, the principle of operation of a voice coil motor is to place the coil in a permanent magnet and move it in the magnetic field through the effect of electromagnetism. The magnetic field generated by the coil is proportional to the magnitude of the current. In contrast to linear motors, no actual contact exists between the mover and the stator of the voice coil motor; thus, less friction is lost. Voice coil motors are often used in fields that require high-speed reciprocation.

C. *Force constant of the voice coil motor and the magnetic field model*

If the length of the threaded coil of the motor is considered to be limited, then the diameter and distance of the coil affect the strength of the magnetic field at any point on the central axis of the coil. If the magnetic field of the coil is far from the magnetic field centre of the permanent magnet, then the force constant of the coil decreases. The distance between the coil and the centre of the magnetic field of the permanent magnet affects the force constant of the voice coil motor. To analyse the magnetic field model, this study first conducted an experiment on the magnetic field of the voice coil motor to determine the force constant of the magnetic field centre and each position.

The force constant of the coil is affected by the permanent magnetic field. Accordingly, if the relative position of the coil and the centre of the permanent magnetic field is limited, the force constant is limited. The force constant in the model can be expressed as follows:

$$K_t(y) = f(F_C, \Delta y, I_C) \quad (2)$$

where y is the position of the linear optical scale of the voice coil motor mover, I_C is the current of the voice coil motor, and Δy is the relative distance between the voice coil motor mover and the stator magnetic field. In the experimental environment of this study, the controller provided a current step signal to the voice coil motor (Fig. 7).

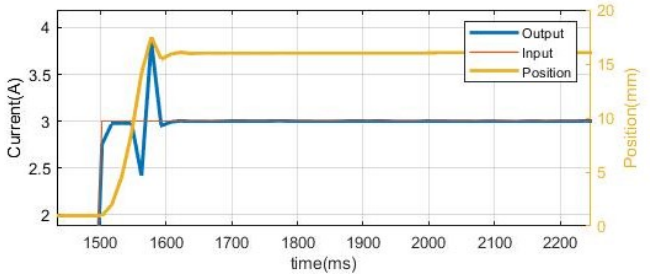

Fig. 7. Relationship between V-step transient response and mover displacement

After the mover coil generates a magnetic field, it generates an opposite force to the magnetic field of the permanent magnet. The kinetic energy of the force drives the mover to ensure that it makes contact with the force sensor. The coil and the permanent magnet no longer produce relative motion after contact. At this instant, the force sensor records data regarding changes in the force. The recorded data can be used as the reference value of finding the force constant. Moreover, the y-axis displacement can be used as the independent variable, and the output current Ic can be used as the control variable, which can be used to derive the output force F_C at different positions Δy in order to derive the force-constant model K_t (Fig. 8).

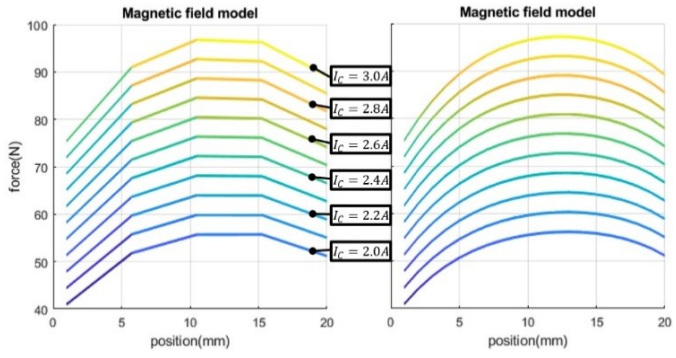

Fig. 8. Force-constant model K_t and curve fitting

D. Curve fitting of the magnetic field model

This study used MATLAB to perform curve fitting for the force-constant model data; thus, the magnetic field model of the voice coil motor could be derived (Fig. 8, right panel). For the voice coil motor used in this experiment, as the magnetic field moved away from the centre point of the coil, the force constant decreased gradually. Only 75% of the centre point remained when the field reached both ends of the coil; this signifies that at the same current, the output force is lower than the expected value. Subsequently, different weights were added in the experiment (0/1/2/3/4/5 kg). After the measurement of the output force, curve fitting was performed with reference to the static resultant force (50 N, as measured by the force sensor; Fig. 9).

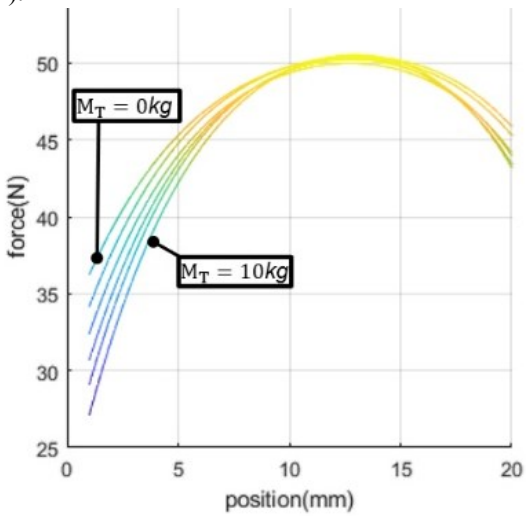

Fig. 9. Influence of load changes on magnetic field curve

The addition of loads was noted to influence the force constant. To facilitate the observation of the influence of the loads on force control performance, this study conducted curve fitting on the data points (Fig. 10).

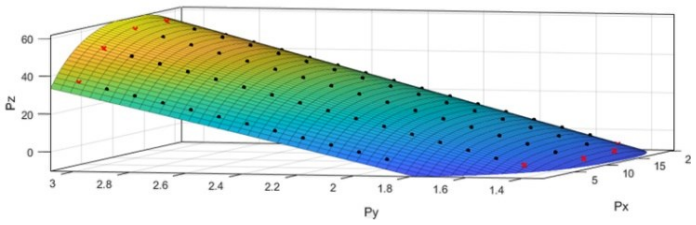

Fig. 10. Curve fitting results for force constant

The simulation results indicated that the contact force optimization method enabled stable and rapid contact operation under changing load conditions and that the control error derived for the same contact force under different loads was improved. To further verify the effectiveness of the optimization method in the control of the voice coil motor, this study also conducted an experiment involving the use of a robotic arm to execute a polishing process.

IV. Experimental Results For Robot Arm Polishing

A. Experimental environment

A robotic arm equipped with the proposed ACF was used to polish a raw egg (Fig. 11). MATLAB (2021b), scanCONTROL Configuration Tools 6.6 (a laser line scanner), and scanCONTROL 3D-View 3.6 (a laser ranger output visualization program) were used in the experiment. The effective stroke of the ACF system was 20 mm. The speed of the robotic arm was 10 mm/s. The egg rotated eccentrically at 0.5 rpm, and the eccentricity of the rotation was more than 5 mm. The maximum gravity tilt angle was 45°. During the polishing process, the contact force was set to 1 N, and the rotating speed of the polishing wheel was 300 rpm. During movement execution processes, the inertial measurement unit and attitude coordinates sent back by the arm were used to calculate the gravity tilt angle to provide the ACF with instant force control.

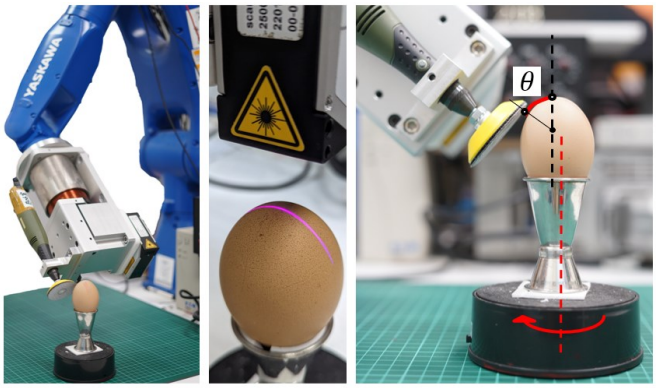

Fig. 11. Experimental process

E. Polishing results

The surface of the egg was inspected after every minute of polishing, as displayed in Fig. 12. The results revealed that the voice coil motor–based ACF and the contact force optimization method maintained the integrity of the egg structure during the polishing operation. The average roughness increased slightly, but it tended to converge centrally. In general, in polishing operations, roughness inevitably becomes stable towards the end of the polishing processes. The surface of an egg is comparable to that of high-quality car sheet metal with regard to the characteristics important for polishing. Accordingly, this study compared the time required for egg polishing with that required for sanding and revealed that egg polishing was faster than sheet metal sanding; this is because eggs are softer than sheet metals. Only a small contact force and a short transient response time is required in egg polishing. Accordingly, the results of this experiment demonstrate that the proposed electromagnetically driven ACF is suitable for high-precision polishing.

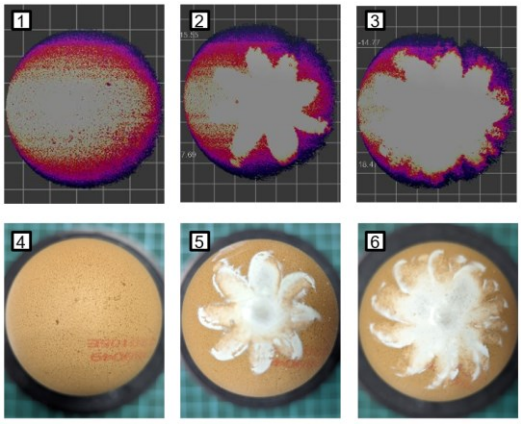

Fig. 12. Polishing results - Software analysis and polishing result

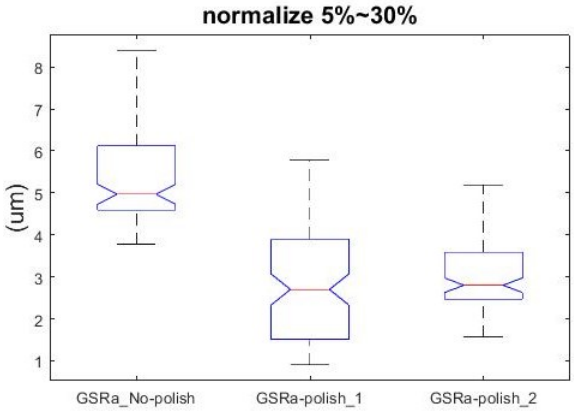

Fig. 13. Polishing results - The box and whisker plot of surface roughness

V. Conclusion

This study proposes an electromagnetically driven ACF for polishing operations. The study established a magnetic field model to improve the contact force quality; this can solve the problem of the nonlinearity of the output force of two interacting magnetic fields in the voice coil motor under varying relative distances and can improve the control performance of the electromagnetic driver under small contact forces, thus improving polishing performance. The experimental results indicate that when a constant load was applied to the mover, the transient response time of the electromagnetic driver was short. Moreover, fewer steady-state errors allow the ACF to maintain high control precision compared with a pneumatic driver, even without the use of a force sensor. The proposed ACF is useful for achieving static or dynamic control for precision polishing.

References

[1] G. Eason, B. Noble, and I. N. Sneddon, “On certain integrals of lipschitzhankel type involving products of bessel functions,” Philosophical Transactions of the Royal Society of London. Series A, Mathematical and Physical Sciences, vol. 247, no. 935, pp. 529–551, 1955.

[2] Y. Chen and F. Dong, “Robot machining: recent development and future research issues,” The International Journal of Advanced Manufacturing Technology, vol. 66, no. 9, pp. 1489–1497, 2013.

[3] D. E. Whitney, “Historical perspective and state of the art in robot force control,” The International Journal of Robotics Research, vol. 6, no. 1, pp. 3–14, 1987.

[4] Q. Xie, H. Zhao, T. Wang, and H. Ding, “Adaptive impedance control for robotic polishing with an intelligent digital compliant grinder,” in International Conference on Intelligent Robotics and Applications. Springer, 2019, pp. 482–494.

[5] Y. Ishida, “Recent development of the passive vibration control method,” Mechanical Systems and Signal Processing, vol. 29, pp. 2–18, 2012.

[6] L. Liao, F. J. Xi, and K. Liu, “Adaptive control of pressure tracking for polishing process,” Journal of manufacturing science and engineering, vol. 132, no. 1, 2010.

[7] D. Zhang and X. Feng, “The technical principle of voice coil actuator,” ZHONGBEI DAXUE XUEBAO ZIRAN KEXUE BAN, vol. 27, no. 3, p. 224, 2006.

[8] S. Morosi and I. F. Santos, “Active lubrication applied to radial gas journal bearings. part 1: Modeling,” Tribology International, vol. 44, no. 12, pp. 1949–1958, 2011.

[9] Y. Kakinuma, K. Igarashi, S. Katsura, and T. Aoyama, “Development of 5-axis polishing machine capable of simultaneous trajectory, posture, and force control,” CIRP Annals, vol. 62, no. 1, pp. 379–382, 2013.

[10] A. E. K. Mohammad and D. Wang, “Electrochemical mechanical polishing technology: recent developments and future research and

industrial needs," The International Journal of Advanced Manufacturing Technology, vol. 86, no. 5, pp. 1909–1924, 2016.
[11] J. Hong, A. El Khalick Mohammad, and D. Wang, "Improved design of the end-effector for macro-mini robotic polishing systems," in Proceedings of the 3rd International Conference on Mechatronics and Robotics Engineering, 2017, pp. 36–41.
[12] D. Wang et al., "A novel mechatronics design of an electrochemical mechanical end-effector for robotic-based surface polishing," in 2015 IEEE/SICE International Symposium on System Integration (SII). IEEE, 2015, pp. 127–133.
[13] M. Schumacher, J. Wojtusch, P. Beckerle, and O. von Stryk, "An introductory review of active compliant control," Robotics and Autonomous Systems, vol. 119, pp. 185–200, 2019.
[14] J.-D. Hsu and Y.-Y. Tzou, "Modeling and design of a voice-coil motor for auto-focusing digital cameras using an electromagnetic simulation software," in 2007 IEEE Power Electronics Specialists Conference. IEEE, 2007, pp. 939–944

H. I. Lin received the M.S. degree in Department of Electrical and Control Engineering from National Chiao Tung University, Hsinchu, Taiwan, in 1999, and Ph.D. degree in Department of Electrical and Computer Engineering from Purdue University, West Lafayette, Indiana, USA, in 2009. He is currently a Professor with National Yang Ming Chiao Tung University, Hsinchu, Taiwan. His current research interests and publications are in the areas of intelligent robot control, machine learning, and artificial intelligence.

Y. H. Chen received the M.S. degree in Graduate Institute of Automation Technology from National Taipei University of Technology, Taipei, Taiwan, in 2022. He is currently a Research Assistant with National Yang Ming Chiao Tung University, Hsinchu, Taiwan. His current research interests are in the areas of robotic polishing and tool design.